

Published in final edited form as:

J Neurosci Methods. 2008 September 15; 174(1): 62–70. doi:10.1016/j.jneumeth.2008.06.036.

Implantable microelectrode arrays for simultaneous electrophysiological and neurochemical recordings

Matthew D. Johnson¹, Robert K. Franklin^{2,3}, Matthew D. Gibson¹, Richard B. Brown³, and Daryl R. Kipke^{1,2}

¹Department of Biomedical Engineering, University of Michigan, Ann Arbor, USA

²Department of Electrical Engineering and Computer Science, University of Michigan, Ann Arbor, USA

³Department of Electrical and Computer Engineering, University of Utah, Salt Lake City, USA

Abstract

Implantable microfabricated microelectrode arrays represent a versatile and powerful tool to record electrophysiological activity across multiple spatial locations in the brain. Spikes and field potentials, however, correspond to only a fraction of the physiological information available at the neural interface. In urethane-anesthetized rats, microfabricated microelectrode arrays were implanted acutely for simultaneous recording of striatal local field potentials, spikes, and electrically-evoked dopamine overflow on the same spatiotemporal scale. During these multi-modal recordings we observed 1) that the amperometric method used to detect dopamine did not significantly influence electrophysiological activity, 2) that electrical stimulation in the medial forebrain bundle (MFB) region resulted in electrochemically-transduced dopamine transients in the striatum that were spatially heterogeneous within at least 200 μm , and 3) following MFB stimulation, dopamine levels and electrophysiological activity within the striatum exhibited similar temporal profiles. These neural probes are capable of incorporating customized microelectrode geometries and configurations, which may be useful for examining specific spatiotemporal relationships between electrical and chemical signaling in the brain.

Keywords

neural probe; amperometry; dopamine; spike recordings; local field potentials; striatum

Introduction

The physiological basis for local field potentials (LFPs) is an increasingly significant question given the involvement of LFPs in neurological disorders (Bragin et al., 2002; Hammond et al.,

© 2008 Elsevier B.V. All rights reserved.

Address correspondence to: Daryl R. Kipke, Department of Biomedical Engineering, University of Michigan, 2149 LBME Building, 1101 Beal Ave., Ann Arbor, MI 48109-2099, PH: (734)-764-3716, fax: (734)-786-0072, e-mail: dkipke@umich.edu.

NOTE: Current address for M. D. Johnson: Department of Biomedical Engineering, Lerner Research Institute, Cleveland Clinic, 9500 Euclid Ave, ND20, Cleveland, OH, 44195 USA

Publisher's Disclaimer: This is a PDF file of an unedited manuscript that has been accepted for publication. As a service to our customers we are providing this early version of the manuscript. The manuscript will undergo copyediting, typesetting, and review of the resulting proof before it is published in its final citable form. Please note that during the production process errors may be discovered which could affect the content, and all legal disclaimers that apply to the journal pertain.

Disclosure

Daryl R. Kipke is a co-founder of NeuroNexus Technologies.

2007), the hemodynamic response of fMRI (Logothetis et al., 2001; Mukamel et al., 2005; Niessing et al., 2005), and neural prosthetic applications (Schwartz et al., 2006). Understanding the rhythmic generation and amplification of LFPs in the intact brain may benefit from techniques that can simultaneously monitor neurotransmitter dynamics. An approach to examine correlations between tonic neurotransmitter concentrations assessed through microdialysis and local field potentials (LFPs) has been suggested previously (Darbin et al., 2006). However, to examine high-frequency oscillations, which are often transient, sampling neurotransmitter levels requires a faster approach such as *in vivo* electrochemistry (Adams, 1976; Boulton et al., 1995).

Previous reports examining both electrochemical and electrophysiological signals in the same preparation have focused on single-unit spike activity and have employed either a ‘serial’ or a ‘parallel’ approach. The former consists of toggling between recording modalities with a single microelectrode (Armstrong-James and Millar, 1984; Cheer et al., 2005; Crespi et al., 1995; Ikeda et al., 1985; Stamford et al., 1993; Williams and Millar, 1990), while the latter involves continuously detecting each modality with separate, closely-spaced microelectrodes (Bickford-Wimer et al., 1991; Hefti and Felix, 1983; Su et al., 1990). The ‘serial’ approach has the advantage of sampling both types of signals from the same location, but it inevitably leads to under-sampling and can result in LFP filtering artifacts that can make concurrent recordings of low-frequency oscillations difficult to interpret. In combination with amperometric techniques, the ‘parallel’ approach resolves these issues, but can be problematic if the microelectrodes for each recording modality are not located within the same microenvironment. Developing a neural probe with precise and closely-spaced microelectrode sites is a well-suited problem for microfabrication (Wise et al., 1970).

Recent advances in microfabrication processes have enabled the development of microelectrode arrays with highly reproducible geometrical and electrical characteristics. These devices have facilitated sampling electrical activity of the same neuron from multiple perspectives (Blanche et al., 2005; Drake et al., 1988) as well as different neurons across multiple microenvironments (Buzsaki, 2004; Csicsvari et al., 2003). Moreover, with certain microelectrode materials such as platinum (van Horne et al., 1990) or carbon (Sreenivas et al., 1996), these arrays are capable of detecting phasic changes in neurotransmitter levels in the extracellular space through electrochemical techniques such as amperometry (Burmeister et al., 2000).

Here, we describe an intracranial, silicon-substrate probe that facilitates concurrent recordings of LFPs and spikes on one set of microelectrodes (Blanche et al., 2005) and detection of extra-synaptic dopamine dynamics on an adjacent set of microelectrodes through constant potential amperometry (Kawagoe and Wightman, 1994; Pennington et al., 2004). These multi-modal probes were implanted in the striatum of urethane-anesthetized rats to examine 1) reciprocal influences of amperometry on neuronal activity, and 2) spatiotemporal characteristics of dopamine efflux and LFP/spike activity following electrical stimulation of the medial forebrain bundle (MFB).

Materials and Methods

Microsensor Array Fabrication

Microfabrication of silicon-substrate probes involved an eight-mask process, including selective boron diffusion in silicon to define the probe geometry; patterned deposition of thin-film dielectrics, traces, and conductors; and subsequent probe-wafer release in ethylenediamine-pyrocatechol (Drake et al., 1988). The devices developed for this study consisted of a single 7-mm long shank with a linear array of microelectrode sites (Fig. 1). Along the shank, the majority of sites alternated between iridium ($177 \mu\text{m}^2$) and platinum (450

μm^2) for transduction of electrophysiological and amperometric signals, respectively. Center to center site separation was 200 μm , which facilitated multi-modal recordings while limiting putative amperometric cross-talk between channels (Yu and Wilson, 2000). Arrays were attached to a 16-channel printed circuit board (PCB) with hot wax. Array bond pads were then wire-bonded with gold wire to the PCB and insulated with a silicone elastomer (MED-4211; Nusil Technology, Carpinteria, CA).

Surgical Procedures

Ten male Sprague-Dawley rats (250–350 g) were anesthetized with an intraperitoneal injection of urethane (1500 mg/kg), placed in a stereotaxic frame with a base heating pad (myneurolab.com, St. Louis, MO), and supplied with a steady flow of oxygen. Heart rate and blood-oxygen levels were monitored with a pulse oximeter. The surgical procedure involved opening three craniotomies including two on the right hemisphere over coordinates for the striatum (AP: 0–2 mm, ML: 1–3 mm) and the medial forebrain bundle (AP: –4.6 mm, ML: 1.4 mm) and one on the left hemisphere (AP: 1–3 mm, ML: 3–4 mm) for placement of an Ag/AgCl wire reference electrode (Paxinos and Watson, 2005). To facilitate probe implantation, dura mater was resected over both right hemisphere craniotomies. A bipolar stimulating electrode (MS308, Plastics One, Roanoke, VA) was then lowered to the MFB target (DV: 7.8–8.1 mm). Reference electrodes were positioned between the dura mater and a piece of saline-soaked gelfoam (Pfizer, New York, NY). Four auxiliary 316SS bone screws were also secured on the contralateral hemisphere with another bone screw placed 1 mm posterior to lambda for an electrophysiological recording ground. The array was then inserted quickly (0.5–1.5 mm/s) into the striatum through a micromanipulator to reduce acute tissue damage (Bjornsson et al., 2006; Johnson et al., 2007). Recordings were made at least 30 minutes after device insertion to allow for tonic dopamine levels to equilibrate. Each rat was maintained in the stereotaxic frame placed inside a Faraday cage. All procedures complied with the NIH guidelines for the care and use of laboratory animals and were approved by the University of Michigan Committee on Use and Care of Animals.

Electrochemical Recordings

Probes were dipped three times in the perfluorinated ion-exchange resin Nafion (Sigma-Aldrich; St. Louis, MO) and dried at 200°C for five minutes to improve selectivity of platinum sites for dopamine (Gerhardt and Hoffman, 2001). Site impedances at 1 kHz after Nafion deposition were $1.611 \pm 0.094 \text{ M}\Omega$ at iridium sites and $0.579 \pm 0.022 \text{ M}\Omega$ at platinum sites. Prior to and after the surgical procedures, each Nafion-coated platinum microelectrode was characterized for its sensitivity to dopamine (Fig. 2A) and selectivity over confounding analytes. In separate solutions of 0.1 M phosphate buffered saline (pH 7.4, warmed to 37°C), the microelectrode arrays were challenged with infusions of dopamine (DA – 20 nM to 50 μM), ascorbic acid (AA – 1 to 200 μM), dihydroxyphenylacetic acid (DOPAC – 1 to 200 μM), and homovanillic acid (HVA – 1 to 200 μM). These analytes were detected through constant potential amperometry at +500 mV in reference to an Ag/AgCl glass body electrode (Kawagoe and Wightman, 1994; Pennington et al., 2004). Devices typically achieved selectivity ratios greater than 100:1 for AA, DOPAC, and HVA and DA detection limits of 200 nM post-implantation, which were defined as current steps with a signal-to-noise ratio greater than three.

In vivo amperometry consisted of applying the same anodic potential versus an AgCl reference electrode and sampling the resulting current at 60 Hz through either a 4-channel potentiostat (Biostat System, ESA, Chelmsford, MA) or a single-channel potentiostat (PGSTAT12 Autolab, Eco Chemie, Utrecht, Netherlands). Experimental stimulation of the MFB began once the non-faradaic charging current at each platinum site had reached approximately 1–5 pA (or ~30–60 minutes post-implantation). Electrochemical measurements were digitized and stored for offline analysis in MATLAB (Mathworks, Natick, MA). Analysis of the arrays' sensitivity

prior to implant and after explant showed a significant decrease in sensitivity from 10.04 ± 0.08 pA/ μ M to 1.72 ± 0.2 pA/ μ M (Fig. 2A–C). Consistent with previous studies, we used the post-implant calibrations for assessing *in vivo* dopamine concentrations (Phillips and Wightman, 2003).

While confirmation that the amperometric currents corresponded exclusively to dopamine was unattainable (Phillips and Wightman, 2003), we did employ metrics to increase our confidence in the detected waveforms including verifying that the sensor selectivity ratios were greater than 100:1 for other oxidizable analytes. *In vivo* experiments comprised of electrically stimulating a fiber bundle containing dopaminergic neurons and subsequent recording in distal regions innervated by those fibers. In addition, we observed increased amplitude and duration in the electrically-evoked signals following intraperitoneal injection of the dopamine uptake inhibitor nomifensine (7–12 mg/kg) (Fig. 2D) (Wightman and Zimmerman, 1990). For striatal implants in which the distal recording site resided in or near the corpus callosum, little to no dopamine signal was detected after MFB stimulation (Fig. 2E). Hence, subtraction of the residual background signal on this site from more distal amperometric signals in striatum removed ‘noise’ common to both microelectrodes, which is an approach similar to the self-referencing technique proposed by (Burmeister and Gerhardt, 2001).

Electrophysiological Recordings and Stimulation

Local field potential and spike recordings were made continuously across seven $177 \mu\text{m}^2$ iridium sites, which were referenced to a bone screw positioned posterior to the cranial lambda mark. The location of this reference was chosen because of its distance from brain regions of high amplitude field potentials that might bias field potential measurements (Berke et al., 2004). For each recording session, Medusa or Pentusa amplifiers sampled voltage-time series data sets at 25 kHz with 16-bit resolution and band-pass filtering from 0.1 to 100 Hz for LFPs and 500 to 5000 Hz for spikes (Tucker-Davis Technologies, Alachua, Florida).

The medial forebrain bundle was stimulated through a bipolar electrode with a biphasic pulse train (10–100 pulses, 10–100 Hz, 2 ms pulse duration, 30–300 μ A, (Wightman and Zimmerman, 1990)) triggered by an RV8 base station (Tucker-Davis Technologies, Alachua, Florida) and delivered through a stimulus isolator (A-M Systems Model 2200, Sequim, WA). Since the duration of stimulation was fixed (1 s), the number of pulses within the stimulation train scaled with the frequency of the stimulation. Identical trials with inter-trial periods of at least 100 s were repeated 5 to 10 times for each location sampled within the striatum (Michael et al., 1987), after which a different set of stimulation parameters were repeated such that the parameter sweep varied randomly among implant depths and animals. Time stamps of stimulation onset were recorded and used to examine peri-event activity.

Statistical Analysis

Current measured at each recording site was converted into dopamine concentration with each site’s post-implant sensitivity to dopamine as shown in Fig. 2. Recordings were analyzed for the maximum stimulation-evoked dopamine concentration across multiple trials. Peak amplitudes were first normalized by subtracting the current 100 ms prior to stimulation onset and then assessing significant differences between trials (ANOVA with subsequent post-hoc Tukey tests, $p < 0.05$).

Power spectral densities of recorded LFPs were calculated to investigate changes in oscillatory activity concurrent with electrically-evoked dopamine overflow. Event-averaged spectrograms of the LFP data were generated in MATLAB utilizing a segmented multi-tapered Fourier transform function (1 s window, 0.5 s steps, $NW=3$, $K=5$) with results averaged across trials (www.chronux.com). Each frequency band of a given spectrogram was baseline-subtracted

with the average spectral response 5–10 s prior to stimulation. Typical response windows were 20 to 50 s in duration.

Unit-spike activity before and after electrical stimulation was sorted in Offline Sorter (Plexon, Dallas, TX) using a combination of automated t-distribution expectation maximization and manual clustering. Inter-spike interval histograms (ISIs) and cross-correlograms were examined for each sorted waveform to verify that sorting did not inadvertently group or divide neurons between sorting clusters. Peri-stimulus time histograms (PSTHs) and raster plots for each sorted waveform were generated in NeuroExplorer (Nex Technologies, Littleton, MA). To examine possible changes in firing rates during constant potential amperometry, PSTHs with 100 ms bins were compared 20 s prior to and 20 s during the applied bias potential for each neuron. Wilcoxon rank-sum tests were then used to assess significant changes in the average firing rates ($p < 0.05$).

Histology

Following each experiment, rats were perfused with 100 mL of 0.1 M PBS followed by 300 mL of a 5% paraformaldehyde solution. Explanted brains were blocked around the striatum and the medial forebrain bundle implants. Striatal blocks were sliced in 10 μm coronal sections with a cryostat, stained for cell nuclei (Hoescht 33342, Invitrogen, Carlsbad, CA) and in some cases also tyrosine hydroxylase (32–2100, Invitrogen) and μ -opioid receptors (ab10275, Abcam, Cambridge, MA), and imaged to locate the probe tracts. MFB blocks were sliced in 50–100 μm sections with a vibratome, stained with cresyl violet, and imaged to determine the final placement of the MFB bipolar electrode.

Results

Effects of constant potential amperometry on spike and local field potential activity

A previous study found that chronoamperometric pulses with amplitudes less than +0.55 V did not influence unit-spike activity (Hefti and Felix, 1983); however, the effects of constant potential amperometry on neuronal activity *in vivo* remain unclear. In our study, microelectrodes sites spaced 200 μm to 2.4 mm from a voltage-biased platinum site were used to record spike and LFP activity during constant potential amperometry. When the electrochemical bias potential was first applied, the adjacent recordings often exhibited a transient electrical artifact lasting 3 to 5 ms. Unlike other amperometric and voltammetric waveforms, however, constant potential amperometry produced no residual artifacts on adjacent or distal microelectrode sites.

Single and multi-unit spike recordings were analyzed for reciprocal effects during constant potential amperometry at +250 mV ($n=32$), +500 mV ($n=25$), and +750 mV ($n=24$). The mean firing rates across at least five trials for each cell were calculated for 20 s prior to and 20 s during the electrochemical recordings. Only microelectrodes spaced 200, 600, and 1000 μm from a voltage-biased platinum microelectrode were used in the analysis. For the large majority of recordings, neuronal activity during amperometry showed no change in average firing rate. At the 250 mV potential, 2/32 neurons had a slight but significant inhibition during amperometry (0.72 Hz to 0.40 Hz, $p=0.032$, and 1.28 Hz to 0.92 Hz, $p=0.024$, Wilcoxon rank-sum test). Only 1/25 cells exhibited a significant change in firing rate during the +500 mV trials (0.25 to 0.58 Hz, $p=0.040$). At +750 mV, 3/24 neurons showed a decrease in firing rate (0.28 to 0.00 Hz, $p=0.008$; 3.38 to 0.78 Hz, $p=0.016$; and 3.67 to 2.07 Hz, $p=0.016$). However, potentials up to +750 mV at individual 450 μm^2 platinum sites did not generally affect neuronal firing rates ($p > 0.05$, two-way ANOVA). In terms of concurrently recorded LFPs, no significant changes in the LFP power spectra were apparent during constant potential amperometry ($p > 0.05$).

Spatiotemporal heterogeneity of electrically-evoked striatal dopamine dynamics

Following repeated MFB stimulation trials, we observed peak striatal dopamine overflow signals with nearly identical responses (Fig. 3). These responses were examined across a range of stimulation intensities and frequencies. Higher stimulation amplitudes evoked progressively larger dopamine overflow with peaks 95% larger at 150–175 μ A than at 100–125 μ A (ANOVA, $p=0.004$, $n=28$ for seven different implants). Increasing stimulation frequency also resulted in detection of greater response magnitudes with the highest magnitudes generated with pulse trains at or above 100 Hz.

The multi-channel potentiostat used in these experiments permitted sampling from only four microelectrodes at any one time, but the probes themselves provided up to eight distinct locations for detecting dopamine dynamics. Multiple 4-channel recording configurations were examined in which spacing between platinum recording sites ranged between 200 μ m to more than 1 mm along the dorsal-ventral axis of striatum. A representative example of these recordings is shown in Fig. 3, in which spatially-heterogeneous dopamine overflow across multiple regions of striatum was observed following electrical stimulation of the MFB. These differences were repeatable for multiple stimulation trials at the same striatal implant depth ($n=5$ per location). Post-implant calibration of the platinum sites showed slight variation in sensitivity between sites; however, both raw amperometric measurements and calibration-converted waveforms demonstrated similar spatial response heterogeneity.

Concurrent recordings of dopamine overflow and striatal LFPs

Since platinum sites were held at a fixed potential, adjacent iridium microelectrodes could readily record local field potentials with no apparent cross-talk between conducting traces. Fig. 4 shows an example of these recordings during MFB stimulation, which induced transient and robust modulation of striatal LFPs. Prior to stimulation onset, striatal LFPs exhibited slow-wave activity (0.1–4 Hz), which was characteristic of urethane anesthesia (Magill et al., 2006) (Fig. 4A). After MFB stimulation, however, activity in this band was suppressed for more than 20 s. These responses were repeatable for consecutive stimulation trials provided that the trials were not performed more than once per minute (Michael et al., 1987). In general, stimulation at 10 Hz (10 pulses) depressed slow-wave activity for only 5 to 10 s, whereas stimulation at 100 Hz (100 pulses) reduced slow-wave activity for 30 to 60 s. In conjunction with these dynamics, the arrays often detected spatially heterogeneous gamma-band activity (40–90 Hz) and as shown in Fig. 4B,C the baseline-subtracted spectrograms, regions with larger amounts of detected dopamine paralleled greater modulation of LFP activity.

Concurrent recordings of dopamine overflow and striatal spike activity

The majority of neurons in the striatum have been described as medium spiny projection cells (90–95%) with spike activity characterized by long-duration action potentials, firing rates less than 5 Hz, and non-bursting activity in the anesthetized state (Gerfen and Wilson 1996). Neuronal activity with these characteristics was readily apparent during recordings with the multi-modal arrays, though the observed proportion of cells of this type was slightly lower (81%, 55 of 68 cells). On occasion, the arrays also recorded other neurons with faster firing rates and bursting activity (19%, 13 of 68 cells).

When firing activity was modulated following MFB stimulation, most responses were excitatory. While the initial increase in firing rate may have resulted from antidromic stimulation (Nieuwenhuys et al. 1982), the prolonged responses were likely due to a different mechanism. Fig. 5A shows an example of two different types of responses recorded simultaneously on the same microelectrode array. The unit in the top row exhibited baseline firing characteristics of a medium spiny cell and an increase in firing rate (0.2 to 4 Hz for approximately 6 s) following MFB stimulation. In this case, an adjacent microelectrode site

recorded an electrochemical dopamine transient with an average peak response of 700 nM with elevated levels lasting for 8.8 s. Other cells exhibited prolonged inhibitory responses following MFB stimulation (Fig 5A, bottom row). For this cell, the decreased firing rate also paralleled an increase in dopamine overflow that was significantly above baseline for 9.6 s.

The same neurons that were modulated at high intensity MFB stimulation also exhibited a dose-dependent relationship to electrical stimulation frequency (Fig. 5B,C). For an example cell with an excitatory response to MFB stimulation, 10 Hz pulse trains did not substantially modulate its firing rate above a 95% confidence interval (dashed line), but 100 Hz stimulation did lead to significant excitation lasting for ~12 seconds. In parallel with these recordings, a negligible electrochemical dopamine signal was detected at 10 Hz stimulation, whereas significantly elevated dopamine levels were apparent following 100 Hz stimulation with durations similar to those observed in the firing rate analysis.

Discussion

We developed a microfabricated microelectrode array for simultaneous recording of electrophysiological and endogenous extra-synaptic dopamine signals. Recordings from these arrays in the striatum of urethane-anesthetized rats revealed spatial heterogeneity of electrically-evoked dopamine and spatiotemporal parallels between recording modalities. While there are reports describing microdialysis measurements with LFP recordings made from electrodes implanted outside (Fried et al., 1999; Ludvig et al., 1992) or inside the microdialysis tubing (Darbin et al., 2006; Obrenovitch et al., 1993), to our knowledge measuring neurotransmitter levels and LFPs at the same spatiotemporal scale through microfabricated arrays is a novel approach. In this parallel scheme, a constant bias potential sufficient to oxidize dopamine was applied independently at multiple platinum sites across the array with currents sampled every 16 ms. This fixed potential permitted the recording of wide-band electrophysiological activity simultaneously on adjacent iridium sites with no residual electrical artifact. The multi-modal concept was integrated into an array of microelectrodes fabricated on a thin silicon-substrate probe (~15 × 80 μm cross-section) (Drake et al., 1988).

A critical, and often overlooked, consideration with *in vivo* electrochemical techniques is the possibility that the applied potentials may influence neuronal activity (Stamford, 1986). Given the experimental challenges of concurrently recording both signal modalities, only a few studies have examined such effects and only in terms of modulations of spike rates (Armstrong-James and Millar, 1984; Crespi et al., 1995; Hefti and Felix, 1983). For example, the studies examining concurrent differential pulse or cyclic voltammetry have suggested that no concomitant changes in firing activity occur (Crespi et al., 1995; Stamford et al., 1993). Another study observed neuronal inhibition (50% of the cells) for chronoamperometric pulses (1 s duration) at potentials between +0.6 and +1.0 V (Hefti and Felix, 1983). Since modulation was not evident at lower voltages in the Hefti and Felix study, the initially high non-faradaic currents (0.5 to 2 μA) at the larger applied potentials may have been responsible for the effects. We show in this study that applying constant potential amperometry to several 450 μm² microelectrode in the striatum, which resulted in picoampere baseline currents, did not significantly modulate striatal activity within 200 μm of the sensors. Whether these findings are consistent in awake-behavioral states or in other brain regions requires further examination. However, we believe the microfabricated arrays presented in this study offer a robust approach for further examination of the spatial distribution of influence, if any, that electrochemical waveforms may have on neuronal activity (Johnson et al., 2005).

The multi-channel recordings showed significant spatial distribution of electrochemical dopamine transients following MFB stimulation with differences evident for microelectrode sites spaced as close as 200 μm apart. This is in agreement with previous studies examining

dopaminergic stores *ex vivo* (Fallon and Moore, 1978; Glowinski and Iversen, 1966) and overflow dynamics *in vivo* with a single carbon fiber along consecutive insertion depths (Bergstrom and Garris, 1999; Garris et al., 1994; May and Wightman, 1989) or at a single implant depth with a cluster of four carbon fibers (Dressman et al., 2002). These reports suggested that electrically-evoked dopamine concentrations could vary over distances less than 100 μm within the striatum given the constraints imposed by diffusion, metabolism, and dopamine transporters (Cragg and Rice, 2004; Peters and Michael, 2000). The increase and decrease of the dopamine signal recorded through the platinum microelectrode sites was of a longer duration than those reported in a previous study using a thin cylindrical carbon fiber microelectrode (Venton et al., 2003), which suggests that a diffusion distance may have been present between the platinum microelectrode surface and release terminals. Narrowing the substrate width or placing the microelectrode sites on the lateral edges of the probe may facilitate closer proximity of the sensors to distal release sites.

The multi-channel measurements also provided evidence that the previously observed dopamine overflow heterogeneity was not simply a manifestation of tissue trauma induced during incremental insertions of a single microsensor (Westerink and De Vries, 1988). It should be emphasized that comparing dopamine responses with multiple microelectrodes requires detailed calibration in terms of sensitivity, response time, and selectivity. Though these metrics will inevitably vary slightly for any microelectrode (Kawagoe et al., 1993), microfabrication processes are designed to limit this variance with reproducible microelectrode geometries and configurations with sub-micron precision (Burmeister and Gerhardt, 2001; Drake et al., 1988; Najafi et al., 1990).

While there is no one technique to identify an *in vivo* amperometric current as deriving exclusively from dopamine, there are ways to increase the confidence in the measurements (Phillips and Wightman, 2003). Selectivity considerations are particularly important since electroactive metabolites are often present in higher extracellular concentrations than their neurotransmitter predecessors (Marsden, 1984). Arrays can include a number of components to improve selectivity. For example, layering of selective diffusion barriers, such as Nafion, over a microelectrode site can limit confounding analyte adsorption or shift its oxidation potential (Gerhardt et al., 1984). Patterns of identical microelectrode geometries on the same neural probe also provide an opportunity for differential recording methods in which a 'reference' site is pre-located in a region devoid of dopaminergic innervation such as in the corpus callosum. An analogous self-referencing approach had been proposed previously to increase signal-to-noise ratios for biosensor recordings (Burmeister and Gerhardt, 2001).

Identification of dopamine overflow can also benefit from certain experimental procedures, including stimulation of dopaminergic projection neurons (somatic or axonal) that directly innervate the targeted recording region (Garris et al., 1997; Yeomans et al., 1988). Additionally, dopamine uptake inhibitors such as nomifensine can be used as selectivity indicators such that the electrically-evoked responses after injection show larger peak amplitudes with extended durations (Wightman et al., 1988). Delivery of such pharmacological agents would benefit from the integration of microfluidic channels within the microfabricated array (Johnson et al., 2003; Rathnasingham et al., 2004). Finally, performing a more selective electrochemical approach such as differential pulse or fast-scan cyclic voltammetry with lower capacitance microelectrode materials, such as glassy carbon or diamond, prior to the multi-modal recordings would provide additional validation of the measurements (Kawagoe and Wightman, 1994).

The parallel recording approach facilitated simultaneous acquisition of electrophysiological signals with no residual electrical artifact. Striatal oscillations are typically smaller than those observed in more laminar brain regions including cortex (Buzsaki and Draguhn, 2004;

Mitzdorf, 1985) and hippocampus (Buzsaki, 2002; Buzsaki et al., 1992). Nevertheless, studies have shown substantial modulation of striatal local field potentials during the sleep-wake transition (Gervasoni et al., 2004), through behavioral tasks (Berke et al., 2004), and in abnormal conditions (Boraud et al., 2005; Costa et al., 2006). We observed modulation of oscillation frequencies following MFB stimulation, particularly in the low (<20 Hz) and occasionally in the gamma (40–90 Hz) bands. These modulations often paralleled the temporal response of dopamine overflow, which may reflect the emergence of synchronized activity within local striatal populations. Indeed, dopamine is thought to have a significant modulatory effect on corticostriatal processing at multiple spatiotemporal scales (Schultz, 2007), which in the depleted state can lead to significant impairment of sensorimotor and motivational circuits as is evident in Parkinson's disease and dopa-responsive forms of dystonia. The multi-modal recording approach demonstrated in this study may thus be useful for investigating the role of neurotransmitters on abnormal oscillation dynamics in neurological disorders (Brown, 2003; Lee et al., 2003; McNamara, 1994).

Future designs incorporating stereotrode and tetrode configurations on the silicon probe should help improve unit isolation, which is important for recording cells with low firing rates or from regions of high neuronal density (Blanche et al. 2005). Moreover, clusters of closely-spaced microelectrodes will be important for studies that seek to robustly correlate spike activity with neurochemical dynamics. Lithographic processes facilitate designing implantable microelectrode arrays with customized recording site placement and substrate shape, high reproducibility of geometrical and electrical characteristics, and smaller cross-section profiles limiting the extent of gross tissue damage that insertion of multiple microwires may cause (Burmeister et al., 2000; Hetke and Anderson, 2002; Wise et al., 2004).

Acknowledgments

This research was supported by a National Institutes of Health NIBIB grant (R21-EB005022) and the NSF Center for Wireless Integrated Microsystems (EEC-9986866). We thank Kat Scott and Charles Wood for technical support; and Jamille Hetke, Ning Gulari, and Brendan Casey for assistance with microfabrication and probe assembly.

References

- Adams RN. Probing brain chemistry with electroanalytical techniques. *Anal Chem* 1976;48:1126A–1138A.
- Armstrong-James, M.; Millar, J. High speed cyclic voltammetry and unit recording with carbon fibre microelectrodes. In: Marsden, CA., editor. *Measurement of neurotransmitter release in vivo*. New York: Wiley: Chichester [West Sussex]; 1984. Chapter 10
- Bergstrom BP, Garris PA. Utility of a tripolar stimulating electrode for eliciting dopamine release in the rat striatum. *J Neurosci Methods* 1999;87:201–208. [PubMed: 11230817]
- Berke JD, Okatan M, Skurski J, Eichenbaum HB. Oscillatory entrainment of striatal neurons in freely moving rats. *Neuron* 2004;43:883–896. [PubMed: 15363398]
- Bickford-Wimer P, Pang K, Rose GM, Gerhardt GA. Electrically-evoked release of norepinephrine in the rat cerebellum: an in vivo electrochemical and electrophysiological study. *Brain Res* 1991;558:305–311. [PubMed: 1782547]
- Bjornsson CS, Oh SJ, Al-Kofahi YA, Lim YJ, Smith KL, Turner JN, De S, Roysam B, Shain W, Kim SJ. Effects of insertion conditions on tissue strain and vascular damage during neuroprosthetic device insertion. *Journal of neural engineering* 2006;3:196–207. [PubMed: 16921203]
- Blanche TJ, Spacek MA, Hetke JF, Swindale NV. Polytrodes: high-density silicon electrode arrays for large-scale multiunit recording. *J Neurophysiol* 2005;93:2987–3000. [PubMed: 15548620]
- Boraud, T.; Brown, P.; Goldberg, JA.; Graybiel, AM.; Magill, PJ. Oscillations in the basal ganglia: the good, the bad, and the unexpected. In: Bolam, JP.; Ingham, CA.; Magill, PJ., editors. *The Basal Ganglia VIII*. New York: Springer; 2005. p. 3-24.

- Boulton, AA.; Baker, GB.; Adams, RN. Voltammetric methods in brain systems. Totowa, N.J: Humana Press; 1995.
- Bragin A, Mody I, Wilson CL, Engel J Jr. Local generation of fast ripples in epileptic brain. *J Neurosci* 2002;22:2012–2021. [PubMed: 11880532]
- Brown P. Oscillatory nature of human basal ganglia activity: relationship to the pathophysiology of Parkinson's disease. *Mov Disord* 2003;18:357–363. [PubMed: 12671940]
- Burmeister JJ, Gerhardt GA. Self-referencing ceramic-based multisite microelectrodes for the detection and elimination of interferences from the measurement of L-glutamate and other analytes. *Anal Chem* 2001;13:1037–1042. [PubMed: 11289414]
- Burmeister JJ, Moxon K, Gerhardt GA. Ceramic-based multisite microelectrodes for electrochemical recordings. *Anal Chem* 2000;72:187–192. [PubMed: 10655652]
- Buzsaki G. Large-scale recording of neuronal ensembles. *Nature neuroscience* 2004;7:446–451.
- Buzsaki G. Theta oscillations in the hippocampus. *Neuron* 2002;33:325–340. [PubMed: 11832222]
- Buzsaki G, Draguhn A. Neuronal oscillations in cortical networks. *Science* 2004;304:1926–1929. [PubMed: 15218136]
- Buzsaki G, Horvath Z, Urioste R, Hetke J, Wise K. High-frequency network oscillation in the hippocampus. *Science* 1992;256:1025–1027. [PubMed: 1589772]
- Cheer JF, Heien ML, Garris PA, Carelli RM, Wightman RM. Simultaneous dopamine and single-unit recordings reveal accumbens GABAergic responses: implications for intracranial self-stimulation. *Proc Natl Acad Sci U S A* 2005;102:19150–19155. [PubMed: 16380429]
- Costa RM, Lin SC, Sotnikova TD, Cyr M, Gainetdinov RR, Caron MG, Nicolelis MA. Rapid alterations in corticostriatal ensemble coordination during acute dopamine-dependent motor dysfunction. *Neuron* 2006;52:359–369. [PubMed: 17046697]
- Cragg SJ, Rice ME. DANCING past the DAT at a DA synapse. *Trends in neurosciences* 2004;27:270–277. [PubMed: 15111009]
- Crespi F, England T, Ratti E, Trist DG. Carbon fibre micro-electrodes for concomitant in vivo electrophysiological and voltammetric measurements: no reciprocal influences. *Neurosci Lett* 1995;188:33–36. [PubMed: 7540274]
- Csicsvari J, Henze DA, Jamieson B, Harris KD, Sirota A, Bartho P, Wise KD, Buzsaki G. Massively parallel recording of unit and local field potentials with silicon-based electrodes. *J Neurophysiol* 2003;90:1314–1323. [PubMed: 12904510]
- Darbin O, Newton L, Wichmann T. A new probe to monitor the effects of drugs on local field potentials. *J Neurosci Methods* 2006;155:291–295. [PubMed: 16497385]
- Drake KL, Wise KD, Farraye J, Anderson DJ, BeMent SL. Performance of planar multisite microprobes in recording extracellular single-unit intracortical activity. *IEEE Trans Biomed Eng* 1988;35:719–732. [PubMed: 3169824]
- Dressman SF, Peters JL, Michael AC. Carbon fiber microelectrodes with multiple sensing elements for in vivo voltammetry. *J Neurosci Methods* 2002;119:75–81. [PubMed: 12234638]
- Fallon JH, Moore RY. Catecholamine innervation of the basal forebrain. IV. Topography of the dopamine projection to the basal forebrain and neostriatum. *J Comp Neurol* 1978;180:545–580. [PubMed: 659674]
- Fried I, Wilson CL, Maidment NT, Engel J Jr. Behnke E, Fields TA, MacDonald KA, Morrow JW, Ackerson L. Cerebral microdialysis combined with single-neuron and electroencephalographic recording in neurosurgical patients. Technical note. *Journal of neurosurgery* 1999;91:697–705.
- Garris PA, Christensen JR, Rebec GV, Wightman RM. Real-time measurement of electrically evoked extracellular dopamine in the striatum of freely moving rats. *J Neurochem* 1997;68:152–161. [PubMed: 8978721]
- Garris PA, Ciolkowski EL, Wightman RM. Heterogeneity of evoked dopamine overflow within the striatal and striatoamygdaloid regions. *Neuroscience* 1994;59:417–427. [PubMed: 8008199]
- Gerhardt GA, Hoffman AF. Effects of recording media composition on the responses of Nafion-coated carbon fiber microelectrodes measured using high-speed chronoamperometry. *J Neurosci Methods* 2001;109:13–21. [PubMed: 11489295]

- Gerhardt GA, Oke AF, Nagy G, Moghaddam B, Adams RN. Nafion-coated electrodes with high selectivity for CNS electrochemistry. *Brain Res* 1984;290:390–395. [PubMed: 6692152]
- Gervasoni D, Lin SC, Ribeiro S, Soares ES, Pantoja J, Nicoletis MA. Global forebrain dynamics predict rat behavioral states and their transitions. *J Neurosci* 2004;24:11137–11147. [PubMed: 15590930]
- Glowinski J, Iversen LL. Regional studies of catecholamines in the rat brain. I. The disposition of [3H] norepinephrine, [3H]dopamine and [3H]dopa in various regions of the brain. *J Neurochem* 1966;13:655–669. [PubMed: 5950056]
- Hammond C, Bergman H, Brown P. Pathological synchronization in Parkinson's disease: networks, models and treatments. *Trends in neurosciences* 2007;30:357–364. [PubMed: 17532060]
- Hefti F, Felix D. Chronoamperometry in vivo: does it interfere with spontaneous neuronal activity in the brain? *J Neurosci Methods* 1983;7:151–156. [PubMed: 6300566]
- Hetke, JF.; Anderson, DJ. Silicon microelectrodes for extracellular recording. In: Finn, WE.; LoPresti, PG., editors. *Handbook of Neuroprosthetic Methods*. Boca Raton, FL: CRC Press; 2002.
- Ikeda M, Miyazaki H, Matsushita A. Simultaneous monitoring of electrochemical and unitary neuronal activities by a single carbon fiber microelectrode. *Jpn J Pharmacol* 1985;37:303–305. [PubMed: 3999480]
- Johnson MD, Franklin RK, Scott KA, Brown RB, Kipke DR. Neural probes for concurrent detection of neurochemical and electrophysiological signals in vivo. *Proceedings of the IEEE Engineering in Medicine and Biology Society* 2005;1:7325–7328.
- Johnson MD, Kao OE, Kipke DR. Spatiotemporal pH dynamics following insertion of neural microelectrode arrays. *J Neurosci Methods* 2007;160:276–287. [PubMed: 17084461]
- Johnson MD, Williams JC, Holecko M, Kipke DR. Chemical sensing capability of MEMS implantable multichannel neural microelectrode arrays. *Proceedings of the IEEE Engineering in Medicine and Biology Society* 2003;4:3333–3336.
- Kawagoe KT, Wightman RM. Characterization of amperometry for in vivo measurement of dopamine dynamics in the rat brain. *Talanta* 1994;41:865–874. [PubMed: 18966011]
- Kawagoe KT, Zimmerman JB, Wightman RM. Principles of voltammetry and microelectrode surface states. *J Neurosci Methods* 1993;48:225–240. [PubMed: 8412305]
- Lee KH, Williams LM, Breakspear M, Gordon E. Synchronous gamma activity: a review and contribution to an integrative neuroscience model of schizophrenia. *Brain Res Brain Res Rev* 2003;41:57–78. [PubMed: 12505648]
- Logothetis NK, Pauls J, Augath M, Trinath T, Oeltermann A. Neurophysiological investigation of the basis of the fMRI signal. *Nature* 2001;412:150–157. [PubMed: 11449264]
- Ludvig N, Mishra PK, Yan QS, Lasley SM, Burger RL, Jobe PC. The combined EEG-intracerebral microdialysis technique: a new tool for neuropharmacological studies on freely behaving animals. *J Neurosci Methods* 1992;43:129–137. [PubMed: 1328772]
- Magill PJ, Pogosyan A, Sharott A, Csicsvari J, Bolam JP, Brown P. Changes in functional connectivity within the rat striatopallidal axis during global brain activation in vivo. *J Neurosci* 2006;26:6318–6329. [PubMed: 16763040]
- Marsden, CA. *Measurement of neurotransmitter release in vivo*. New York: Wiley; 1984.
- May LJ, Wightman RM. Heterogeneity of stimulated dopamine overflow within rat striatum as observed with in vivo voltammetry. *Brain Res* 1989;487:311–320. [PubMed: 2786444]
- McNamara JO. Cellular and molecular basis of epilepsy. *J Neurosci* 1994;14:3413–3425. [PubMed: 8207463]
- Michael AC, Ikeda M, Justice JB Jr. Mechanisms contributing to the recovery of striatal releasable dopamine following MFB stimulation. *Brain Res* 1987;421:325–335. [PubMed: 3500755]
- Mitzdorf U. Current source-density method and application in cat cerebral cortex: investigation of evoked potentials and EEG phenomena. *Physiological reviews* 1985;65:37–100. [PubMed: 3880898]
- Mukamel R, Gelbard H, Arieli A, Hasson U, Fried I, Malach R. Coupling between neuronal firing, field potentials, and fMRI in human auditory cortex. *Science* 2005;309:951–954. [PubMed: 16081741]
- Najafi K, Ji J, Wise KD. Scaling Limitations of Silicon Multichannel Recording Probes. *IEEE Trans Biomed Eng* 1990;37:1–11. [PubMed: 2303265]

- Niessing J, Ebisch B, Schmidt KE, Niessing M, Singer W, Galuske RA. Hemodynamic signals correlate tightly with synchronized gamma oscillations. *Science* 2005;309:948–951. [PubMed: 16081740]
- Obrenovitch TP, Richards DA, Sarna GS, Symon L. Combined intracerebral microdialysis and electrophysiological recording: methodology and applications. *J Neurosci Methods* 1993;47:139–145. [PubMed: 8100599]
- Paxinos, G.; Watson, C. *The rat brain in stereotaxic coordinates*. Burlington: Elsevier Academic; 2005.
- Pennington JM, Millar J, CP LJ, Owesson CA, McLaughlin DP, Stamford JA. Simultaneous real-time amperometric measurement of catecholamines and serotonin at carbon fibre 'dident' microelectrodes. *J Neurosci Methods* 2004;140:5–13. [PubMed: 15589328]
- Peters JL, Michael AC. Changes in the kinetics of dopamine release and uptake have differential effects on the spatial distribution of extracellular dopamine concentration in rat striatum. *J Neurochem* 2000;74:1563–1573. [PubMed: 10737613]
- Phillips PEM, Wightman RM. Critical guidelines for validation of the selectivity of in-vivo chemical microsensors. *Trac-Trend Anal Chem* 2003;22:509–514.
- Rathnasingham R, Kipke DR, Bledsoe SC Jr, McLaren JD. Characterization of implantable microfabricated fluid delivery devices. *IEEE Trans Biomed Eng* 2004;51:138–145. [PubMed: 14723503]
- Schultz W. Multiple dopamine functions at different time courses. *Annu Rev Neurosci* 2007;30:259–288. [PubMed: 17600522]
- Schwartz AB, Cui XT, Weber DJ, Moran DW. Brain-controlled interfaces: movement restoration with neural prosthetics. *Neuron* 2006;52:205–220. [PubMed: 17015237]
- Sreenivas G, Ang SS, Fritsch I, Brown WD, Gerhardt GA, Woodward DJ. Fabrication and characterization of sputtered-carbon microelectrode arrays. *Anal Chem* 1996;68:1858–1864.
- Stamford JA. In vivo voltammetry: some methodological considerations. *J Neurosci Methods* 1986;17:1–29. [PubMed: 3528683]
- Stamford JA, Palij P, Davidson C, Jorm CM, Millar J. Simultaneous real-time electrochemical and electrophysiological recording in brain-slices with a single carbon-fiber microelectrode. *J Neurosci Methods* 1993;50:279–290. [PubMed: 8152239]
- Su MT, Dunwiddie TV, Gerhardt GA. Combined electrochemical and electrophysiological studies of monoamine overflow in rat hippocampal slices. *Brain Res* 1990;518:149–158. [PubMed: 2390719]
- van Horne CG, Bement S, Hoffer BJ, Gerhardt GA. Multichannel semiconductor-based electrodes for in vivo electrochemical and electrophysiological studies in rat CNS. *Neurosci Lett* 1990;120:249–252. [PubMed: 2293112]
- Venton BJ, Zhang H, Garris PA, Phillips PE, Sulzer D, Wightman RM. Real-time decoding of dopamine concentration changes in the caudate-putamen during tonic and phasic firing. *J Neurochem* 2003;87:1284–1295. [PubMed: 14622108]
- Westerink BH, De Vries JB. Characterization of in vivo dopamine release as determined by brain microdialysis after acute and subchronic implantations: methodological aspects. *J Neurochem* 1988;51:683–687. [PubMed: 3411321]
- Wightman RM, Amatore C, Engstrom RC, Hale PD, Kristensen EW, Kuhr WG, May LJ. Real-time characterization of dopamine overflow and uptake in the rat striatum. *Neuroscience* 1988;25:513–523. [PubMed: 3399057]
- Wightman RM, Zimmerman JB. Control of dopamine extracellular concentration in rat striatum by impulse flow and uptake. *Brain research* 1990;15:135–144.
- Williams GV, Millar J. Concentration-dependent actions of stimulated dopamine release on neuronal activity in rat striatum. *Neuroscience* 1990;39:1–16. [PubMed: 2089272]
- Wise KD, Anderson DJ, Hetke JF, Kipke DR, Najafi K. Wireless implantable microsystems: High-density electronic interfaces to the nervous system. *P IEEE* 2004;92:76–97.
- Wise KD, Angell JB, Starr A. An integrated-circuit approach to extracellular microelectrodes. *IEEE Trans Biomed Eng* 1970;17:238–247. [PubMed: 5431636]
- Yeomans JS, Maidment NT, Bunney BS. Excitability properties of medial forebrain bundle axons of A9 and A10 dopamine cells. *Brain Res* 1988;450:86–93. [PubMed: 3261193]

Yu PG, Wilson GS. An independently addressable microbiosensor array: What are the limits of sensing element density? *Faraday Discussions* 2000:305–317. [PubMed: 11197487]

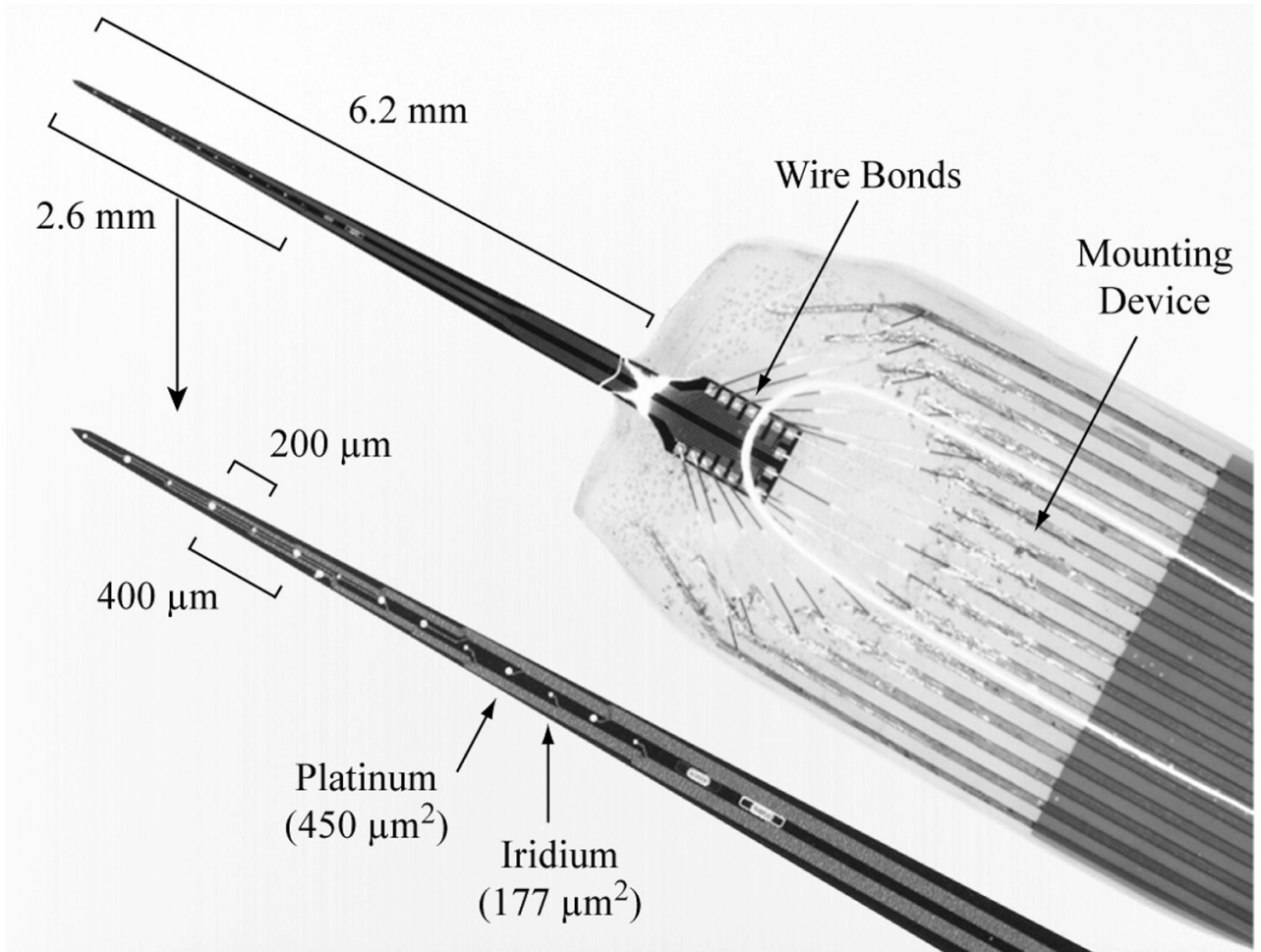
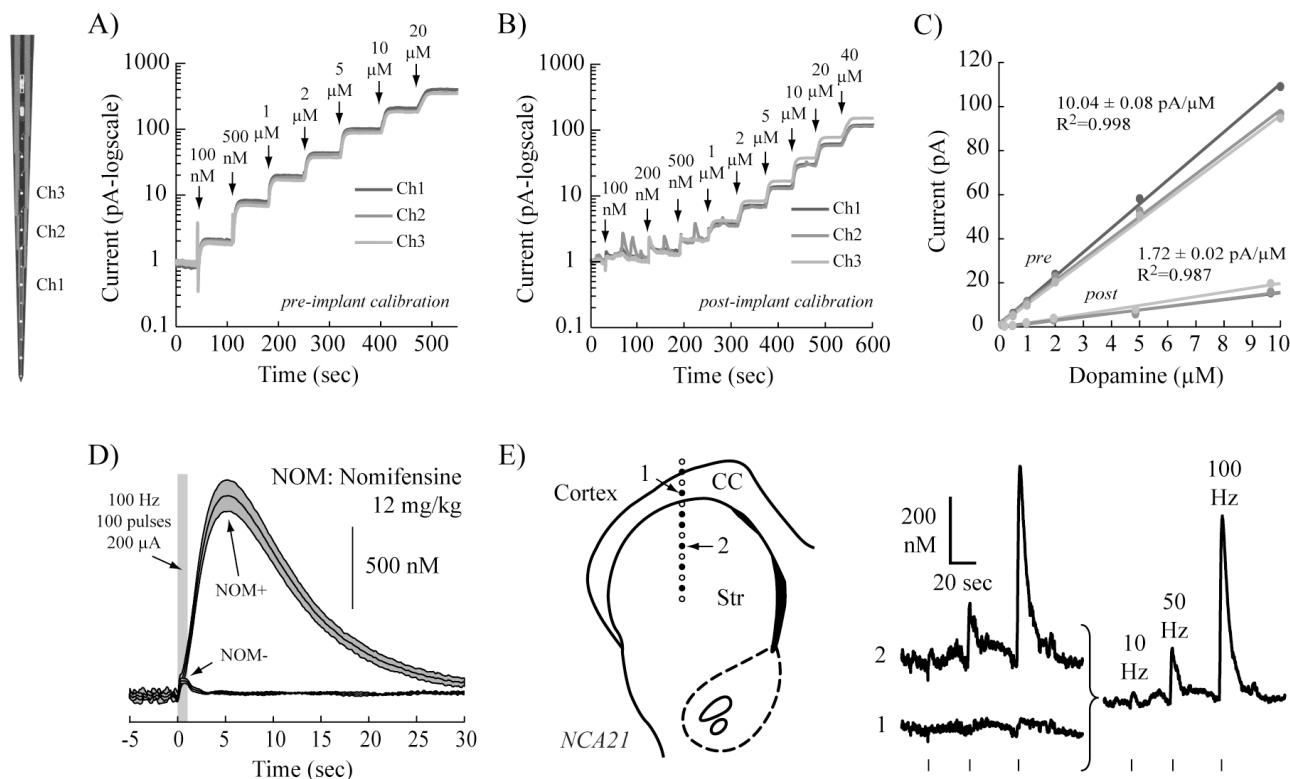


Fig. 1.

Linear microelectrode arrays implanted in rat dorsal striatum recorded unit-spike and local field potential activity on iridium sites ($177 \mu\text{m}^2$) with adjacent platinum sites ($450 \mu\text{m}^2$) used for measuring electrochemical dopamine overflow signals through constant potential amperometry. Arrays were fabricated from a boron-doped, silicon substrate with metal contacts and phosphorus-doped polysilicon traces insulated with a multi-layer stack of silicon dioxide and silicon nitride.

**Fig. 2.**

Interfacial dopamine concentration was transduced at a platinum microelectrode with the constant potential amperometry technique, which involved applying a +500 mV potential with respect to an AgCl electrode. Simultaneous calibration across four channels of the array was performed (A) prior to and (B) after implantation with dopamine solution concentrations ranging from 100 nM to 20 μ M. (C) *In vivo* amperometric recordings were transformed into a dopamine concentration with the post-implant calibration fits. Although sites were sensitive to dopamine after probe explantation, the sensitivity was decreased (paired t-test, $p=0.013$, $n=4$). (D) To verify that the electrically-evoked *in vivo* electrochemical signals corresponded to changes in extra-synaptic dopamine concentrations, rats were injected i.p. with a dopamine uptake inhibitor (nomifensine, 12 mg/kg). Response curves represent an average of five trials with standard errors indicated by the gray fills. (E) MFB stimulation did not elicit detectable dopamine transients when a microelectrode site was positioned in the corpus callosum (CC), which contrasted with the large peaks observed simultaneously in the striatum (Str). Shown are three stimulation trials for 1-s long consecutive pulse trains using frequencies of 10, 50, and 100 Hz (150 μ A, 2 ms duration biphasic waveforms). Subtraction of the two recordings decreased common noise between the two platinum microelectrodes.

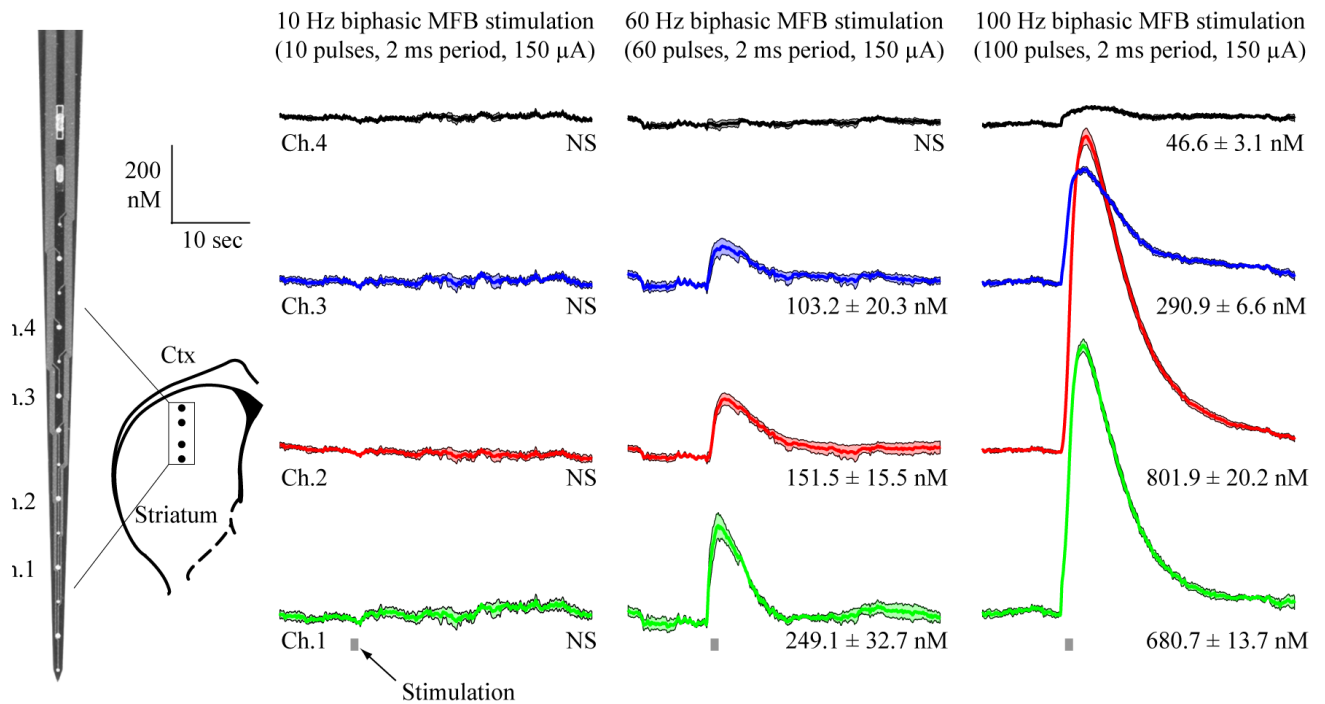


Fig. 3. Concurrent electrochemical recordings across microelectrode sites within the striatum were characterized by spatially heterogeneous responses following MFB stimulation. Response curves exhibited different peak dopamine levels on sites as close as 200 μ m and their magnitudes depended on stimulation frequency. Each trace corresponds to an average of five trials with fill bars indicating standard errors and gray bars indicating stimulus duration. Recordings reflect the presence of nomifensine (10 mg/kg).

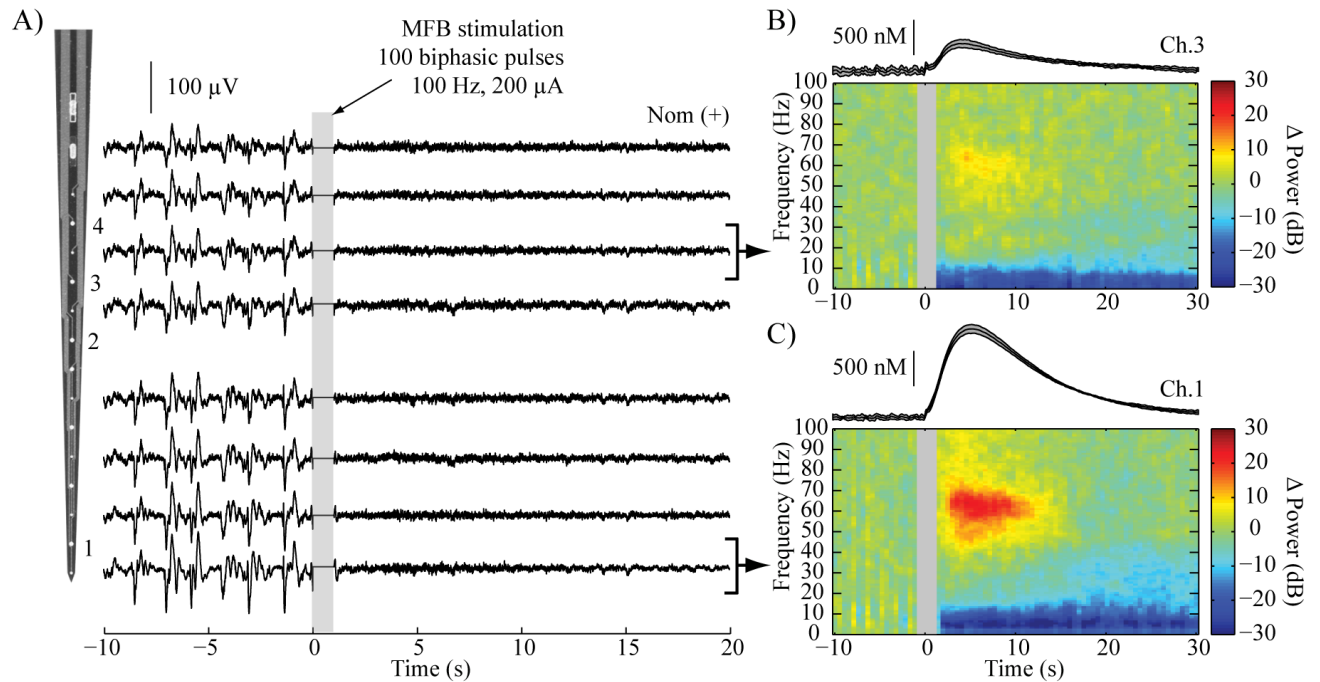
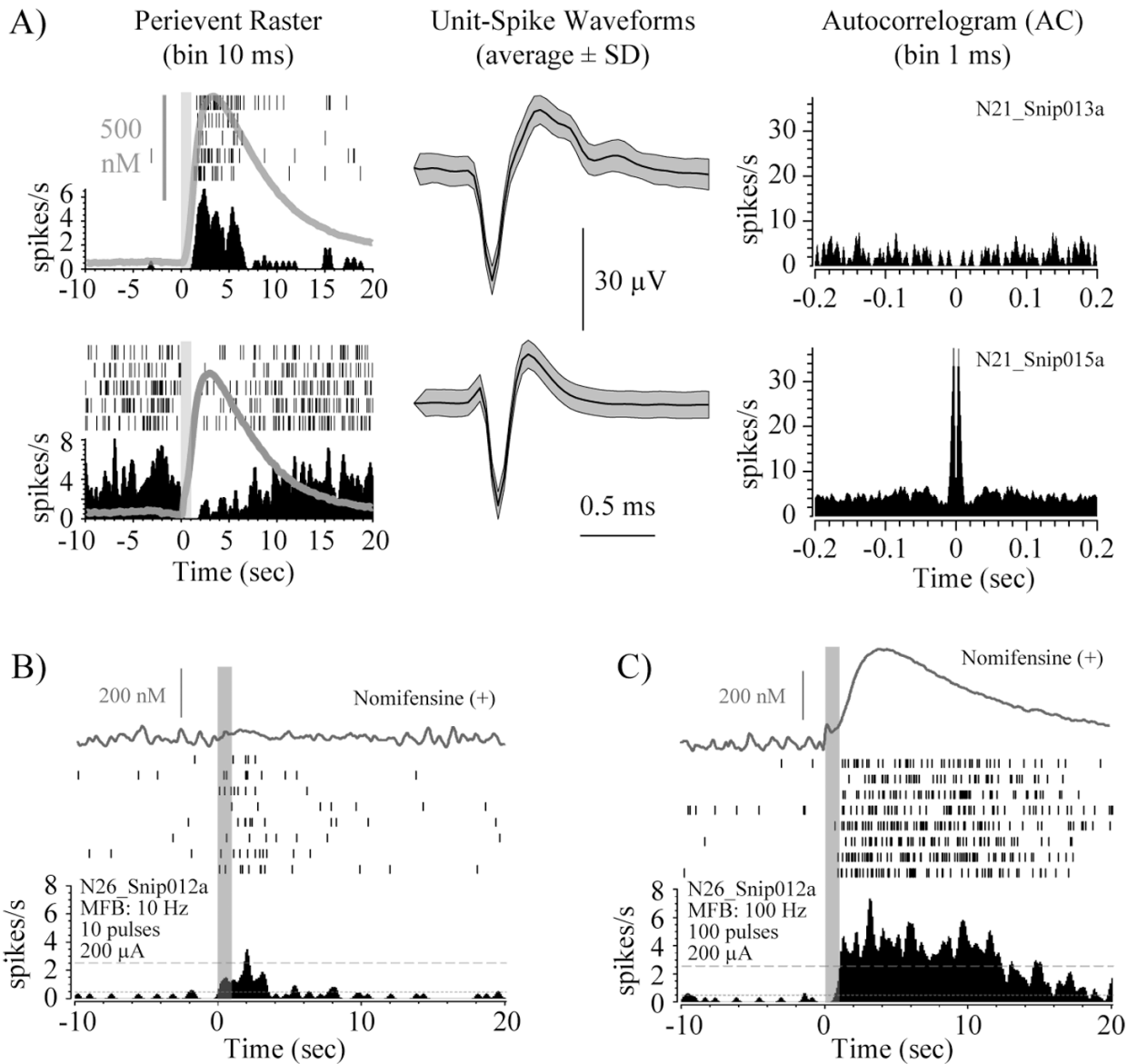


Fig. 4. MFB stimulation elicited local field potential modulation in striatum. (A) The figure shows an example recording session sampled continuously during electrochemical recordings for dopamine on adjacent sites (indicated by numbers 1–4 next to the probe). Following MFB stimulation (indicated by the gray rectangle), slow-wave activity was suppressed considerably and coincided with the emergence of higher frequency activity. (B,C) Event-averaged spectrograms showed significant modulation in the 0–20 Hz and 40–90 Hz bands following stimulation ($n=5$ trials). Above each plot is the event-averaged dopamine response recorded on an adjacent site. Recordings reflect the presence of nomifensine (10 mg/kg).

**Fig. 5.**

Responses to MFB stimulation evoked distinct changes in striatal spike activity as shown in representative examples of neurons recorded simultaneously along an implanted array. (A) This neuron responded with an excitatory response (top row) that paralleled the duration of elevated dopamine overflow. Other neurons (bottom row) exhibited an inhibitory response, which also paralleled dopamine overflow. This particular neuron exhibited a higher incidence of bursting than the neuron shown in the top row as indicated by the autocorrelograms. Recording modalities were separated by 200 μ m. MFB stimulation consisted of a 100 pulse, 100 Hz train of 2 ms duration biphasic waveforms at 150 μ A amplitude. (B, C) An example of neuronal firing rates and dopamine overflow depending on stimulation frequency for a striatal neuron excited during MFB stimulation. Both dopamine overflow and neuronal firing rates were smaller in magnitude and shorter in duration during randomized trials at (B) 10 Hz than at (C) 100 Hz. Recordings reflect the presence of nomifensine (10 mg/kg). Dashed lines

represent 95% confidence intervals. Stimulation artifacts prevented including spikes during the 100 Hz stimulation train in the analysis.